Rational Estimation Method for Internal Pressure
Due to Dry Bulk Cargo during Vertical Acceleration

Research Institute, Research and Development Division, ClassNK
Kuwano Lab., Institute of Industrial Science (IIS), The University of Tokyo

1. INTRODUCTION

In the transportation of dry bulk cargos such as iron ore powder, nickel ore, etc., not only the external pressure of waves, but also the internal pressure of the cargo caused by ship acceleration accompanying ship movement act on the hull. Due to friction between particles, dry bulk cargos have shear friction resistance and display complex behaviors. Unlike shipping containers and other solid cargos, dry bulk cargos show fluidity, but a change in the structural response has been suggested, in that the strain of double-bottom frame members in past measurements of actual ships was smaller than when dry bulk cargos were regarded as a liquid cargo [1].

The ClassNK *Rules for the Survey and Construction of Steel Ships*, *Part C* [1] specifies the loads acting on dry bulk cargos during vertical acceleration as shown in the following formulae (1) and (2) (Fig. 1). Formulae (1) and (2) were established based on estimation formulae for loads associated with liquid cargos, considering friction between particles and the inner surface of the hull. Although the results of past measurements of actual ships [2] and the results of model tests [3-5] suggested that the friction of the particles contributes to internal pressure by dry bulk cargos, rules were specified on the safe side in view of the remaining uncertainties concerning the mechanism and effects.
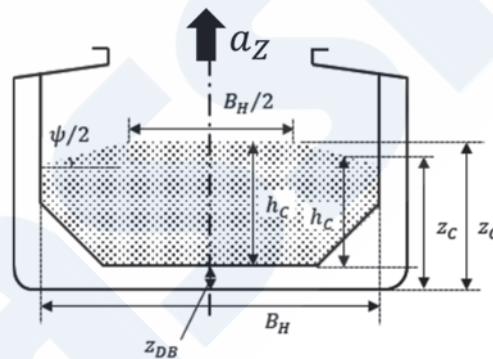
Fig. 1   Bulk cargo carrier [1]

$$P = K_c \rho_c (g + a_z) h_c \qquad (1)$$

$$K_c = \cos^2 \alpha + (1 - \sin \psi) \sin^2 \alpha \qquad (2)$$

P: Pressure acting on a cargo hold loaded with dry bulk cargo,
K_c: Coefficient of static earth pressure,
ρ_c: Density of the dry bulk cargo (t/m^3),
g: Acceleration of gravity (m/s^2),
a_z: Vertical acceleration of ship (m/s^2),
h_c: Cargo loading height (m),
α: Inclination angle to the horizontal of the panel under consideration,
ψ: Angle of repose of the dry bulk cargo.

Based on the background outlined above, the Society conducted research on pressure due to dry bulk cargos. According to the research by the Society to date, it was suggested [9] that changes in the structural response are caused by a redistribution of

loads called the "arching effect [6-8]." The arching effect is a phenomenon that is known in the civil engineering field.

As shown in Fig. 2 (a) (trapdoor experiment), the arching effect is a phenomenon that occurs on the descent of part of the region (called the "floor block" in the figure) supporting a dry bulk cargo, and an arch of particles is formed and the load is redistributed along that arch. The arching effect occurs by the following process: First, when the floor block descends, the particles in the area near the floor block located above the descending floor block also descend with the floor block, as shown in Fig. 2 (b), but more distant particles from the floor remain at the same height, without following the descending floor. The particles that do not descend form a particle arch, which is supported by the action of interparticle friction, and as a result, the load is redistributed toward the roots of the arch.

(a) Trapdoor apparatus　　　　(b) Contour of descent
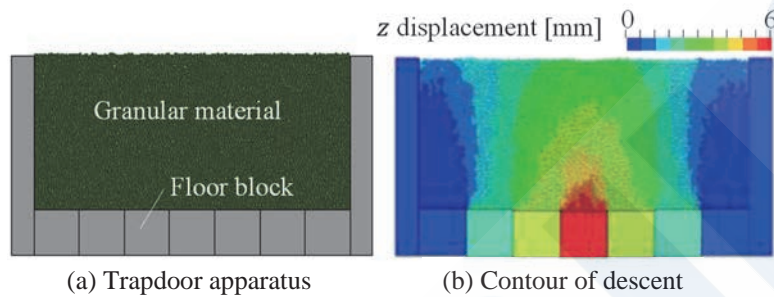
Fig. 2　Arching effect in trapdoor experiment

However, because the arching effect in ships is different from that in civil engineering in the following respects, the Society carried out a basic experimental study and a study by numerical analysis.

(1) It is necessary to consider the interaction of changes in the deflection of a ship's bottom plates accompanying ship motion and redistribution of the load by the arching effect.

(2) Ships are affected by repeated disturbances due to ship motion.

(3) The arching effect in a ship does not occurs in ground having an infinite extension, but rather, in a cargo loaded in the cargo holds, and thus is affected by the ship's construction, including the double bottom structure, ship sides, etc.

This article reports the concept of an oscillation test using an elastic bottom plate, and a preliminary study by DEM-FEM coupled analysis carried out prior to the test.

2.　APPROACH

As the approach of this paper, the principle of the numerical analysis and the experimental study will be explained.

2.1　DEM-FEM Coupled Analysis

As noted above, in order to study the arching effect that occurs in dry bulk cargos in a ship's hold, it is necessary to perform a coupled analysis considering the interaction of the cargo and the ship. In this paper, we used a DEM-FEM coupled analysis in which the behavior of the material (i.e., cargo) particles is obtained by the discrete element method (DEM), and the deformation of the vessel is solved by the finite element method (FEM). The general-purpose software LS-DYNA was used in this analysis.

In DEM [10], the cargo particles are expressed by discrete elements in the form of rigid spheres, and an equation of motion is solved using the contact force between particles as an external force. The contact in the normal and tangential directions is formulated by a spring-dashpot model, and the contact force is calculated from the contraction of the spring, which corresponds to the contact between the elements. For the tangential direction, the frictional force based on Coulomb friction is used.

A bidirectional coupled analysis of the discrete elements and finite elements can be carried out by deformation of the finite elements by the load received from the discrete elements, followed by transmission of the contact force to the discrete elements in the next step.

Table 1 shows the values of the particle parameters used here. In a preliminary analysis [11], an angle of repose of 30.3° was measured as the angle at which the particles begin to move when a container filled with particles is inclined. In an analysis simulating the triaxial compression test, the internal friction angle was 20.0° and cohesion was 5.0 kPa.

Table 1　Physical properties of particles

Property	Value
Coefficient of friction between discrete elements	0.25
Coefficient of friction between discrete elements and shells	0.25
Radius of discrete elements (mm)	3.0
Young's modulus of discrete elements (MPa)	71600
Poisson's ratio of discrete elements	0.23
Density of discrete elements (t/mm^3)	7.6×10^{-9}

2.2　Experimental Study

2.2.1　Oscillation Apparatus

As joint research with the Institute of Industrial Science (IIS), the University of Tokyo, an oscillation experiment using an elastic bottom plate was carried out to evaluate the arching effect with respect to vertical motion. This paper introduces the concept of the test apparatus. A duralumin plate with a thickness of 1.0 mm was used as the bottom plate to enable adequate deflection while avoiding plastic deformation during oscillation. So as not to impede the deformation of the bottom plate, the bottom plate deformation was measured by using a sheet-type electromagnetic pressure sensor having a 40.0 mm square pressure-receiving surface area and a thickness of 0.45 mm.

Although earth pressure gauges or load cells are frequently used in conventional earth pressure measurements, there was concern that those devices might affect the deformation of the bottom plate. The sheet-type sensor was considered appropriate for use in this test apparatus, as it is lightweight and thin, and the sensor itself can deform together with the bottom plate.

Since there are very few examples of measurement of earth pressure during vertical motion with an elastic bottom plate, the trapdoor experiment described in section 2.2.2 was performed prior to the experiment with the above-mentioned apparatus.

2.2.2　Trapdoor Experiment

Because studies of the arching effect in the civil engineering field are normally carried out by discrete dropping of the bottom plate, continuous descent of the bottom plate, like the motion that occurs during deflection of the inner bottom plate of a ship, has not been studied. Therefore, prior to the oscillation test using the above-mentioned apparatus, the effect of the descent shape on the arching effect was examined using a trapdoor test device.

The trapdoor experiment was conducted at the Institute of Industrial Science, the University of Tokyo. Because this paper will only present an outline of the test, the reader should refer to Hirano et al. (2023) [12] for details.

The test setup is shown in Fig. 3. Rigid aluminum blocks are arranged at the bottom of the device and are lowered by motor drive. The amount of descent of the respective blocks is 6.0 mm in the center (Fig. 4, Nos. 11-15), 4.0 mm in the two adjoining areas (Fig. 4, Nos. 6-10 and 16-20) and 2.0 mm at the two edges (Fig. 4, Nos. 1-5 and 21-25). The load was measured using load cells arranged under the blocks.
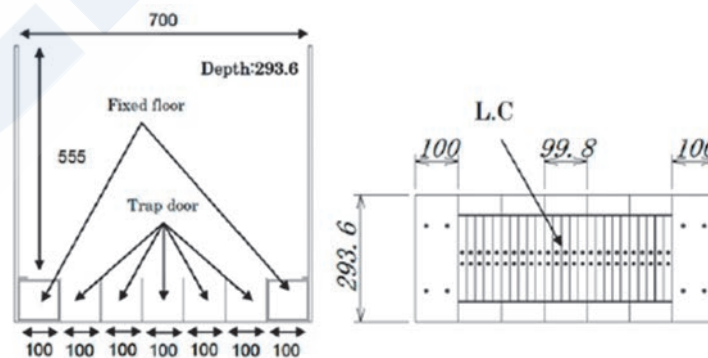
Fig. 3　Setup of trapdoor experiment [11]
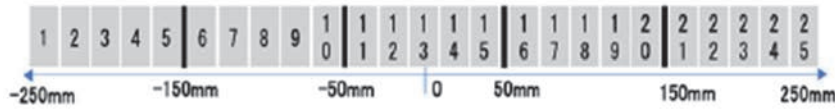
Fig. 4　Load evaluation points in trapdoor experiment [11]

Fig. 5 shows the time history of load changes with respect to the descent of the center block. In the central area, the load decreases rapidly corresponding to block descent. In the two adjoining blocks, the load increases until descent of around 2.0 mm, but then begins to decrease, and the load at the two edges increases gradually. As shown in the load distribution in Fig. 6, no difference in the load due to displacement can be seen in the initial stage, but after descent, the arching effect can be seen, and it was found that the distribution profile depends on the final state. In addition, a condition in which the load increases near the block boundary could also be seen.
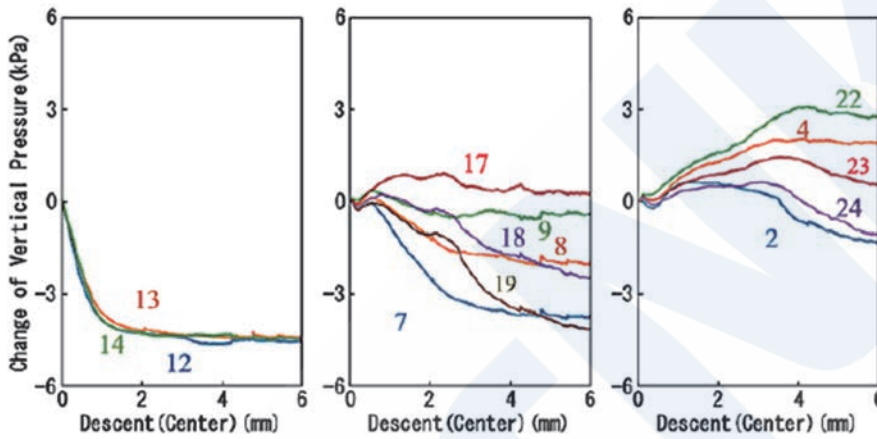
Fig. 5　Time history of load in trapdoor experiment (Case C) [12]
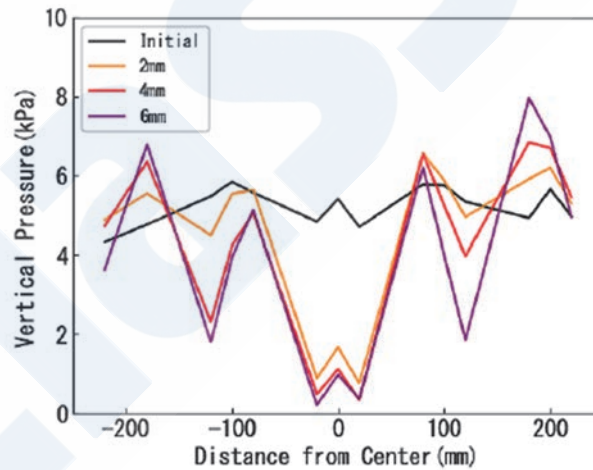
Fig. 6　Load distribution in trapdoor experiment (Case C) [12]

In addition to the above study, the factors in the arch forming conditions were also investigated. When the cargo loading height h_c was changed in order to investigate the relationship between the cargo loading height h_c and breadth B, an arch was formed when $h_c/B \geq 0.40$. With small grain diameters, it was suggested that an arch with a wide breadth is formed by very slight displacement. In addition, the pressure measured by the load cells and the sheet-type sensor were compared, and no large differences between the two were observed. Therefore, we plan to conduct ongoing research on measurement of dynamic response using the oscillation test.

3. DEM-FEM COUPLED ANALYSIS

A condition similar to the deformation of a ship inner bottom plate could be confirmed in the trapdoor experiment described above, although a discrete dropping condition was used in that experiment. An arch also formed above the descending blocks in a separate DEM analysis simulating the trapdoor experiment, confirming that redistribution of the load occurs. This chapter introduces the results of a verification of the arching effect with the elastic bottom plate in which a DEM-FEM coupled analysis was used.

3.1 Arching Effect in Elastic Bottom Plate

With the trapdoor experiment apparatus, an arch is formed when the rigid blocks are forcibly displaced. In a ship, on the other hand, deformation of the bottom plate occurs due to loading from the cargo accompanying ship motion. To consider this interaction, a DEM-FEM coupled analysis was carried out using a vessel with an elastic bottom plate. Because this paper is limited to an outline, please refer to Yanagimoto et al. (2022) [9] for details.

The analysis model is shown in Fig. 7. Because this is a quasi two-dimensional model in which a very short length of the hold was extracted, rigid walls were provided fore and aft as boundary conditions for continuity, and the friction coefficient between the fore and aft walls and particles was set at 0. The walls were assumed to be rigid bodies, and the inner bottom plate was modeled as an elastic body.

First, after self-weight was loaded and the model stabilized, acceleration a_z in the vertical upward direction was applied to the rigid part of the vessel, causing motion in one direction. a_z was set at 0.3 times the acceleration of gravity g.
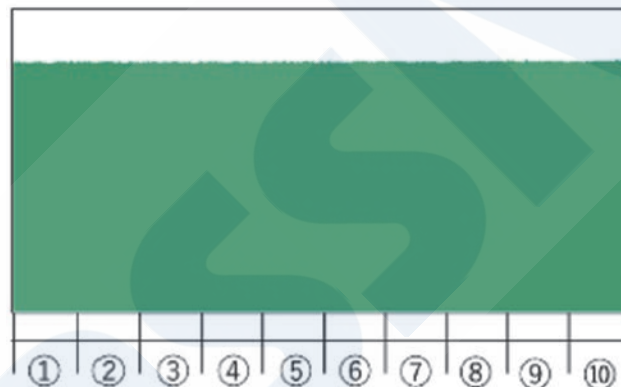
Fig. 7   Load evaluation points of bottom plate [9]

The load distribution is shown in Fig. 8. In this figure, the load is calculated as the force ratio, that is, the pressure in the region being evaluated to the average pressure of the entire bottom plate. In the case of the highest arching effect, the average value of the force ratio acting on the bottom plate was 0.85 times at the vessel center (Fig. 8, ⑤⑥), which forms the inner side of the arch, while a force ratio of 1.2 times acted at the ends of the arch (Fig. 8, ①⑩).
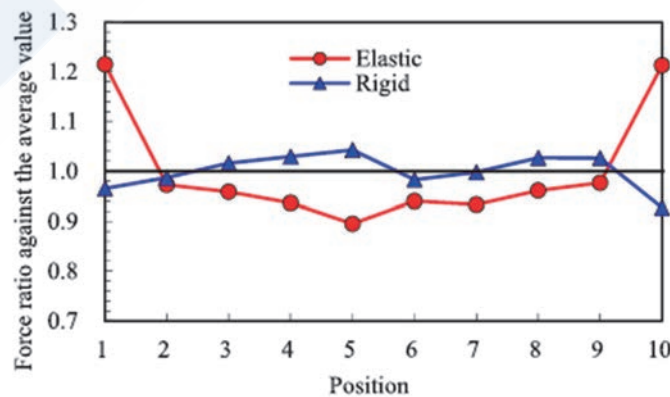
Fig. 8   Load distribution in bottom plate [9]

The ratio of the cargo loading height h_c and vessel breadth B also showed a tendency close to that of the trapdoor experiment in section 2.2.2, as an arch formed when $h_c/B \geq 0.33$. As h_c/B decreases, the arching effect becomes smaller. It was also found that there were no differences when the cargo particle radius was 1.5, 2.0 or 3.0 mm, and the Young's modulus and Poisson's ratio of the bottom plate had no effect on the arching effect.

3.2　Effect of Nonuniform Rigidity of Bottom Plate

In the trapdoor experiment, an arch was formed due to discrete deformation by the rigid blocks, and concentration of the load to the areas near the fixed block boundary could be seen. On the other hand, load concentration in the inner side of the arch was not observed in the elastic bottom plate model in section 3.1. Although a simplified bottom plate had been used in section 3.1, actual ship bottom plates display complex deformation, which includes not only the overall deformation of the total breadth region of the hold, but also superimposed local deformation between girders. Therefore, in this chapter, the influence of the arching effect caused by local deformation on the arching effect due to overall deformation was investigated.

Fig. 9 shows the analysis model, in which elastic shell elements simulating a double bottom and girders were added to the inner bottom plate. Here, a_z was increased monotonously up to 0.15 times the acceleration of gravity g (a_z=0.15 g). The particle parameters and other conditions were the same as those in section 3.1.
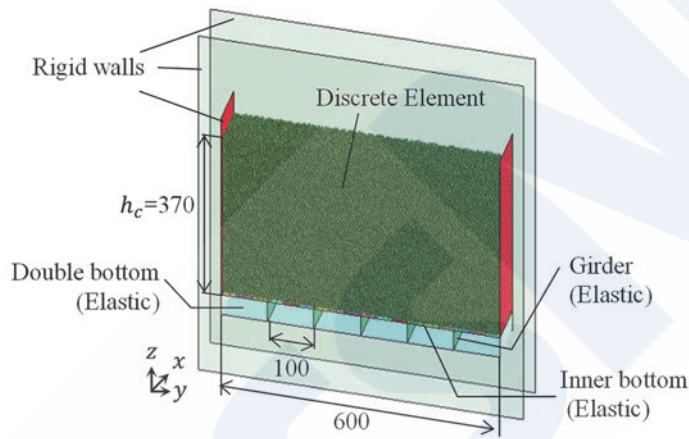
Fig. 9　Model with girders

The analysis results are presented in the following. Fig. 10 shows the contour of force chain at a_z=0.15 g. "Force chain" refers to a visualization technique which shows the force in the direction of principal stress acting on a particle obtained from the contact force with surrounding elements [13]. A large force chain means there is continuity in the magnitude and the direction of principal stress to nearby particles. From Fig. 10, it can be understood that an arch having the same span as the breadth of the ship's hold is formed, and small arches straddling the girders are also formed on the inner side of the arch spanning the hold breadth.
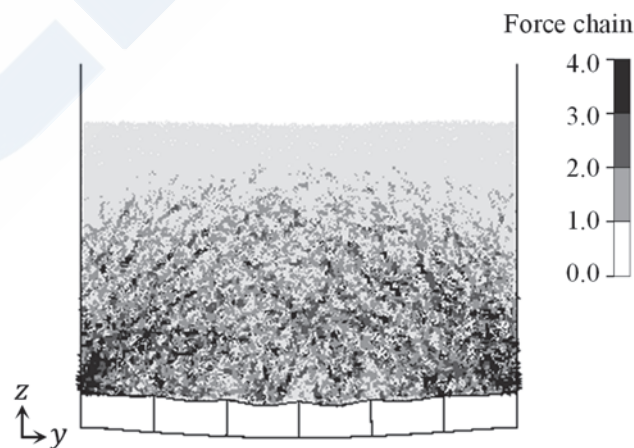
Fig. 10　Contour of force chain

As shown in Fig. 11, deflection occurred in the shape of superimposed overall deformation and local deformation. At the midpoints between girders, the increment of deflection due to dynamic loads is small, and it is thought that local arches were formed with the midpoints as the roots of the arches. In the load distribution in Fig. 12, the loads are concentrated at the midpoints between the girders, which are thought to be the positions of the roots of the local arches, rather than directly above the girders. This is consistent with an estimation based on the force chain and the deflection of the bottom plate.

In addition, in the load distribution in Fig. 12, it is suggested that the effects of the load distribution by the total arch and the distribution by the local arches are superimposed. Thus, it can be conjectured that arching effects occur and are manifested in a superimposed state, even in complex shapes like those of actual ship structures.
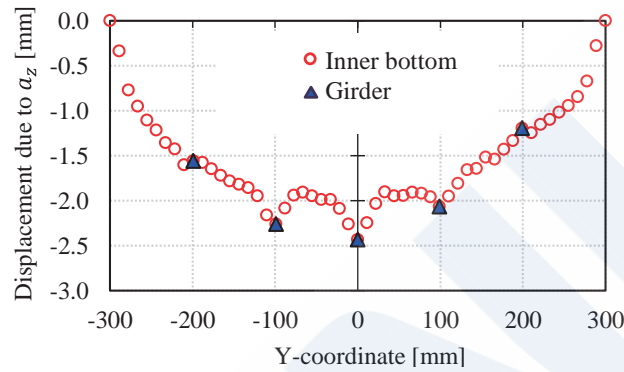
Fig. 11　Increment of deflection caused by vertical acceleration a_z
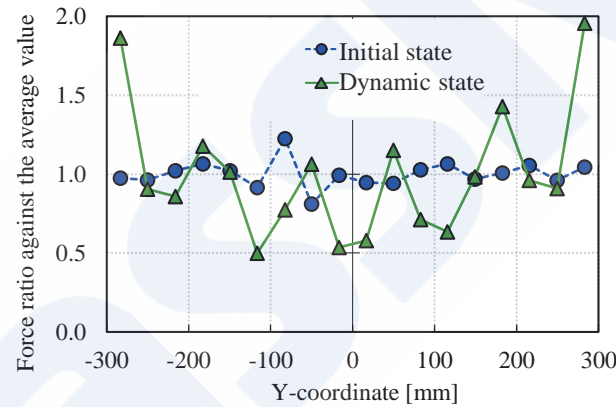
Fig. 12　Load distribution

3.3　Effect of Aspect Ratio of Bottom Plate in 3-Dimensional Vessel

Up to the previous section, this paper has introduced the results of an evaluation of the arching effect in the 2-dimensional state when a section with a very short length was extracted. However, longitudinal deflection also occurs in actual inner bottom plates. This suggests the possibility that the arch is formed not only in the transverse direction, but also in the longitudinal direction, which may influence the load distribution. Therefore, the arching effect caused by 3-dimensional deformation of the bottom plate was investigated using the vessel shown in Fig. 13.
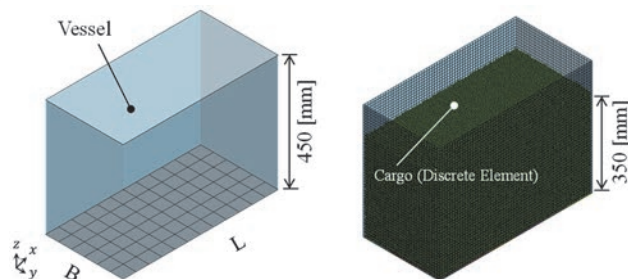
Fig. 13　3-dimensional model

Based on the fact that the ratio of the cargo loading height h_c and vessel breadth B contributes to the conditions for arch formation and arch descent, the relationship between the aspect ratio of the bottom plate and the load distribution is evaluated when the ratio of the length of the vessel bottom plate L and the bottom plate aspect ratio L/B was varied from 1.0 to 2.0, as shown in Fig. 14. As excitation, unidirectional vertical acceleration increasing monotonously up to a_z=0.3 g was applied. The side walls were modeled using rigid shell elements, and the bottom plate was modeled using elastic shell elements.
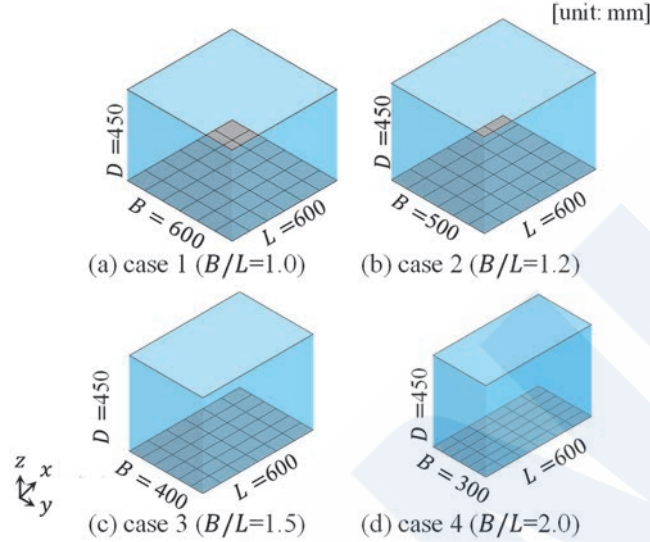
Fig. 14　FE models of cases examined

As the distribution of the dynamic loads in Cases 1 to 4 with different vessel bottom plate aspect ratios L/B at a_z=0.3 g, Fig. 15 shows the distribution in the vessel longitudinal L direction, and Fig. 16 shows the distribution in the vessel transverse B direction. In all cases, the distribution has been normalized by the average values.

In the longitudinal distributions shown in Fig. 15, the load at the center is lower than the average value in all cases. At the edges, the load in Case 1 (square bottom plate) is larger than the average value, while in the other cases, the load is close to the average.

In the transverse distributions shown in Fig. 16, the load at the center is lower than the average value in all cases. At the edges, however, the load is larger than the average value, indicating that the load is concentrated at the edges. In Case 1 with the square bottom plate, the load is approximately the same in the transverse direction, but in the other cases (Cases 2-4), in which the aspect ratio exceeds 1.0, larger loads act in the transverse direction. In addition, the load concentration at the transverse edges increases as the aspect ratio L/B becomes larger, that is, as the bottom plate becomes longer and narrower.
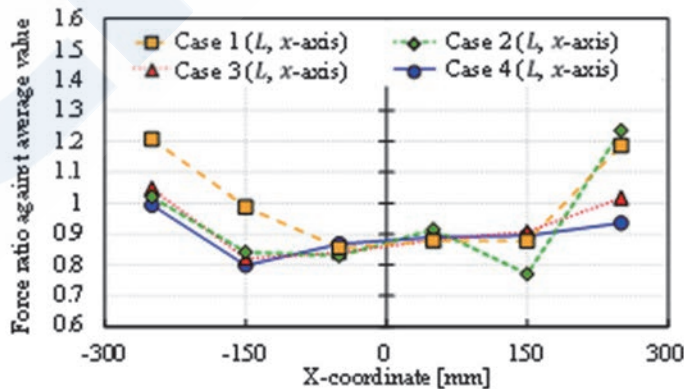
Fig. 15　Load distributions in vessel longitudinal L direction in Cases 1 to 4 with different vessel bottom plate aspect ratios L/B (a_z=0.3 g)
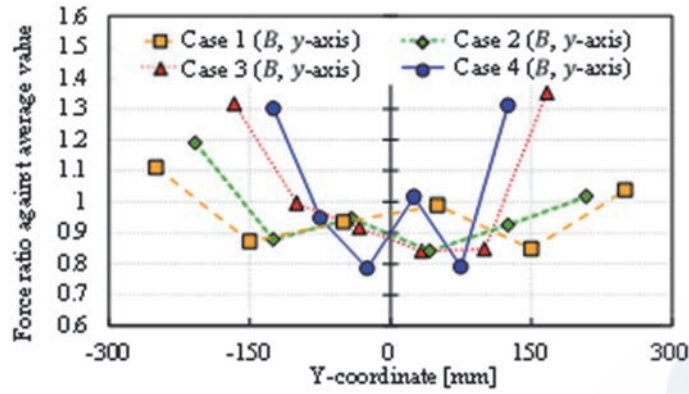
Fig. 16　Load distributions in vessel transverse B direction in Cases 1 to 4 with different vessel bottom plate aspect ratios L/B (a_z=0.3 g)

The cause of the differences in the strength of the arching effect depending on the aspect ratio is considered as follows: A schematic diagram of the arch structure is shown in Fig. 17. When an arch supports a load, in addition to a vertical reaction force, a horizontal reaction force H also occurs at the two ends of the arch [14, 15].
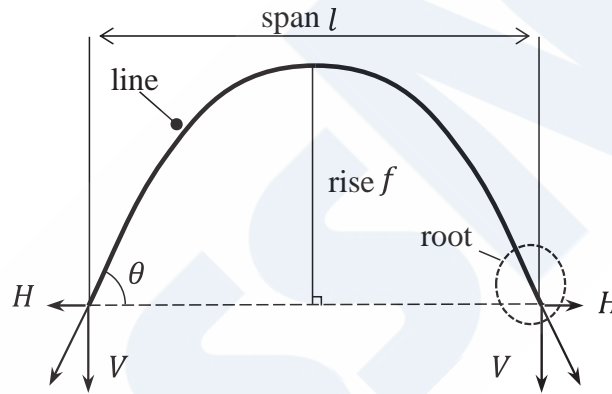
Fig. 17　Arch structure

This horizontal reaction force is supported by the side walls or the particles on the outer side of the arch. Fig. 19 shows the results of an investigation of the pressures (p_L^{lateral}: lateral pressure on sidewall at root of arch in lengthwise direction, p_B^{lateral}: lateral pressure on sidewall at root of arch in breadthwise direction, p_L^{vertical}: vertical pressure on bottom plate at arch root in lengthwise direction, p_B^{vertical}: vertical pressure on bottom plate at arch root in breadthwise direction) when a_z=0.3 g in the region shown in Fig. 18. According to Fig. 19, the lateral pressure is roughly the same in both directions, independent of the aspect ratio, but as the aspect ratio becomes larger, the loads positioned on the roots of the arch in the direction of the short side become larger. This appears to occur because, assuming the same horizontal reaction force acts, the longitudinal arch, which has a smaller arch breadth relative to the arch length, largely supports the vertical reaction force. This tendency is the same as the tendency of the result that, at the same h_c, a small vessel breadth displayed a stronger arching effect in an experiment using a trapdoor model in previous research [8].
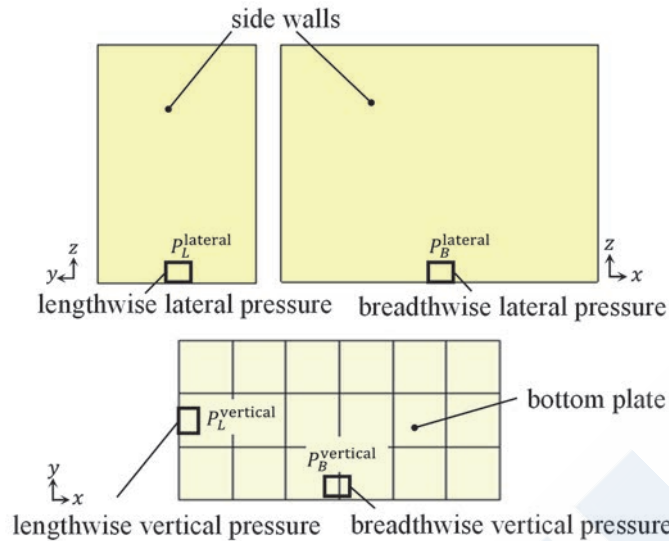
Fig. 18　Load measurement regions of sidewall and bottom plate
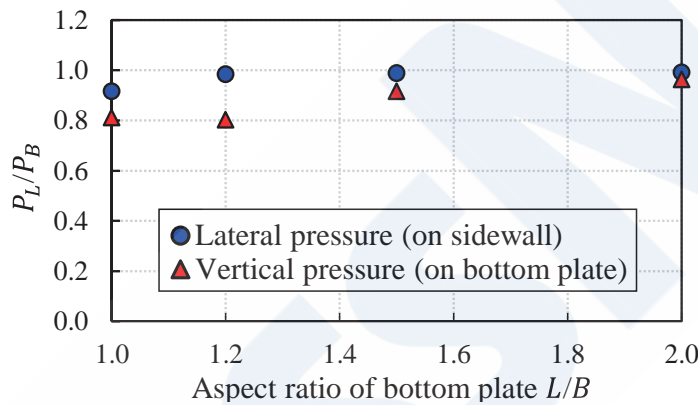
Fig. 19　Relationship of bottom plate aspect ratio and ratio of loads in short and long side directions

4.　CONCLUSION AND FUTURE OUTLOOK

Although it had been pointed out that dry bulk cargos generate smaller loads that those caused by liquid cargos under the same vertical acceleration of a ship, the mechanism had not been clarified. Therefore, the Society carried out research to elucidate this issue.

Based on a survey of the literature and the results of analyses in previous research, the difference between dry bulk cargos and liquids was considered to be due to the arching effect that occurs in dry bulk cargos. Since the interaction of the motion of the cargo particles and deformation of the ship's bottom plate should be taken into account, an evaluation was conducted by an oscillation experiment using a vessel with an elastic bottom plate and DEM-FEM coupled analysis. This paper has introduced those studies, which were carried out as the first steps toward solving this practical problem.

The studies described in this paper clarified the facts that the ratio of the cargo loading height and the vessel breadth has an influence on the arching effect, the arching effects due to local deformation and overall deformation are superimposed in the case of a bottom plate with nonuniform rigidity, and the aspect ratio of the bottom plate also has an effect.

Because more rational structural design is expected to be possible by considering the arching effect, the authors plan to conduct model tests in connection with dynamic response and study the conditions for arch formation and collapse on a continuing basis, with the aim of providing feedback to the Society's *Rules for the Survey and Construction of Steel Ships*.

REFERENCES

1) Nippon Kaiji Kyokai (ClassNK): Rules for the Survey and Construction of Steel Ships, Part C Hull Construction and Equipment, Chapter 1, General Hull Requirements, 2024.

2) Y. Kuramoto, et al.: Full Scale Measurements on Ore Pressure and Practical Design Aspects, J. Soc. Nav. Archit. Jpn., Vol. 1987, No. 162, 1987.

3) Y. Tanaka, et al.: Experimental Study on Pressure Loads Induced by Granular Cargos, J. Soc. Nav. Archit. Jpn., Vol. 1999, No. 186, pp. 445-453, 1999.

4) Y. Tanaka, et al.: Experimental Study on Pressure Loads Induced by Granular Cargos, – Second Report: Evaluation Methods of Bulk Cargo Pressure – , J. Soc. Nav. Archit. Jpn., No. 192, pp. 713-721, 2002.

5) K. Toh, et al.: Study on Estimation Method of Ore Pressure Utilizing Coupling Analysis of DEM and FEM, J. Jpn. Soc. Nav. Archit. Ocean Eng., No. 28, pp. 63-74, 2018.

6) R.L. Handy: The Arch in Soil Arching, Journal of Geotechnical Engineering, 111 (3) 302-318, 1985

7) K. Terzaghi et al.: Soil Mechanics in Engineering Practice, Third Edition, Wiley Interscience, 100-141, 1996

8) S.U. Ali et al.: Particle-scale insight into soil arching under trapdoor condition, Soils and Foundations, 60 (5), 1171-1188, 2020

9) F. Yanagimoto et al.: Numerical investigation of dry bulk cargo load during ship vertical motion, Ocean Eng., 266 (3), 112970, 2022

10) C. O'Sullivan: Particle Discrete Element Modelling: A Geomechanics Perspective, CRC Press, 2011

11) W. Tsuruta, et al.: Evaluation of the Particle-Wall Friction Effects on Dry Bulk Cargo Loads using Transverse Acceleration Using DEM, J. Jpn. Soc. Civ. Eng., Vol. 80 (2024) No. 15, 23-15025, 2024.

12) R. Hirano et al., Experimental investigation of the effect of granular arching under trapdoor condition on the load acting on the bottom plate, 10th Pan Asian Association of Maritime Engineering Societies Forum, C-7-01, pp. 1-9, 2023

13) J.F. Peters et al.: Characterization of force chains in granular material, Phys. Rev. E., 72, 041307, 2005

14) H. Watanabe: Introduction to Design Calculations for Reinforced Concrete and Prestressed Concrete/23, Concr. J., Vol. 14 No. 4 pp. 64-72, 1976

15) A.V. Makarov and S.A Kalinovsky: Methods of regulating thrust in design of arch bridges, IOP Conf. Series: Materials Science and Engineering 451 (2018) 012054, 2018